With a little help from computer-aided drug design

New antitumor agents as tubulin polymerization inhibitors

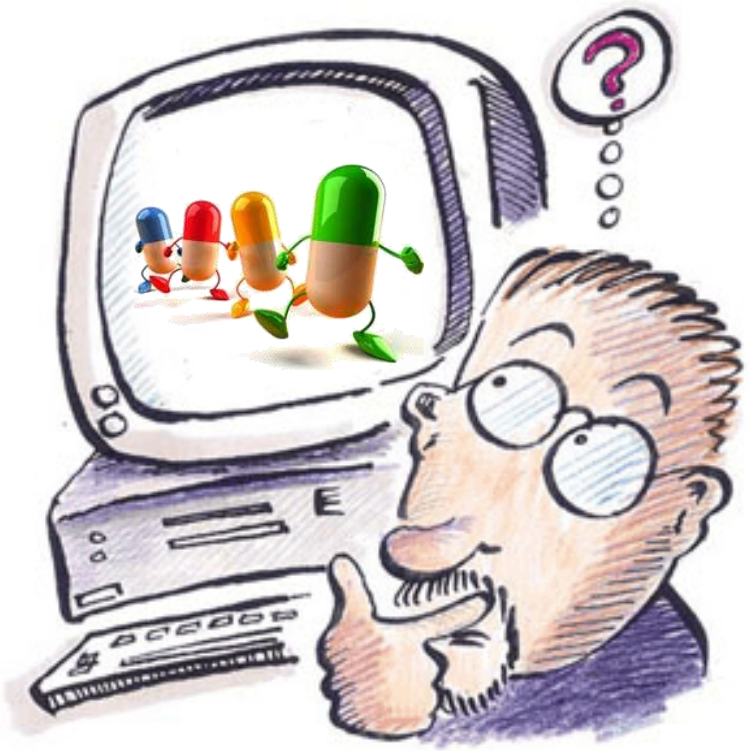

Dr. **ŠČ!** Robert Vianello

Laboratory for the Computational Design and Synthesis of Functional Materials

Ruđer Bošković Institute

Zagreb, Croatia

robert.vianello@irb.hr

Computer-Aided Drug Design

Structure and function of biological systems

- Substrate and inhibitor binding in the active site
- Catalytic and inhibition mechanisms
- Receptor activation, deuterium isotope effects
- Mutated enzymes

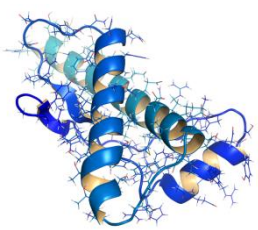

Design of new materials

- Optical chemical sensors and sensing materials
- Catalysts, formulations, ionic liquid gels, DES solvents
- Strong organic superacids and superbases
- Antioxidants

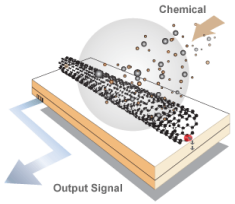

Reaction mechanisms in organic chemistry

- Nucleophilic/electrophilic aditions/subtitutions
- Acid-base reactions
- Rearrangement reactions in mass spectrometry

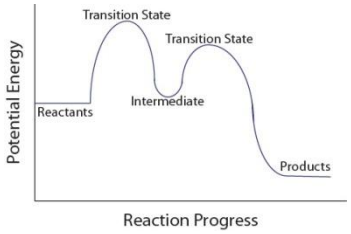

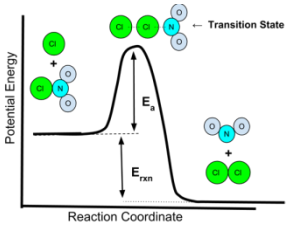

Structure and properties of small molecules

- Organometallic compounds, metal complexes
- Degradation processes
- Spectroscopies in condensed phase

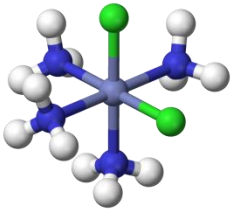

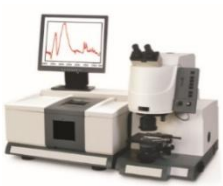

Experiment

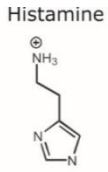

Versus

Theory

Drug Design

Computer-Aided Drug Design (CADD)

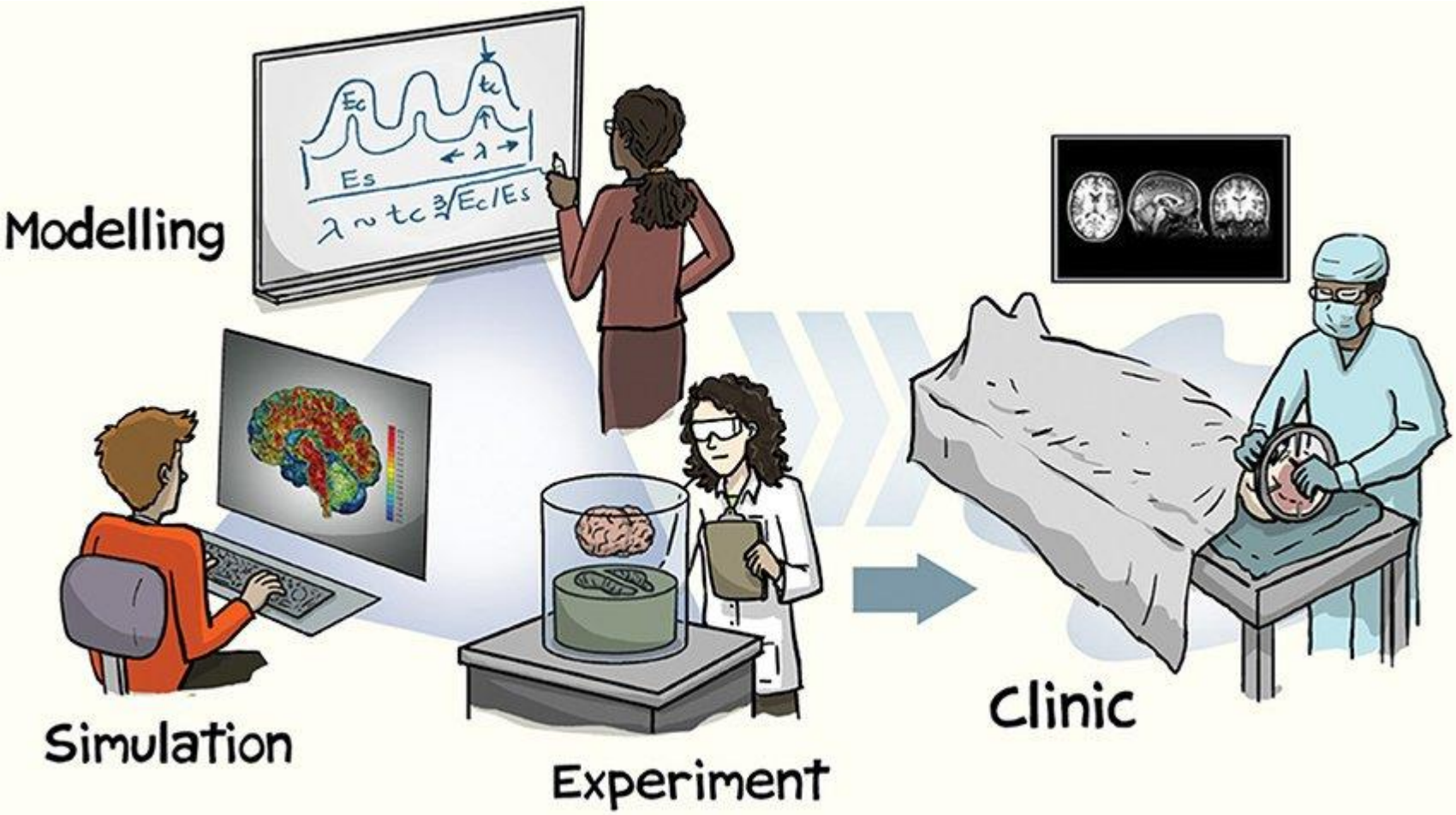

Computer-Aided Drug Design (CADD)

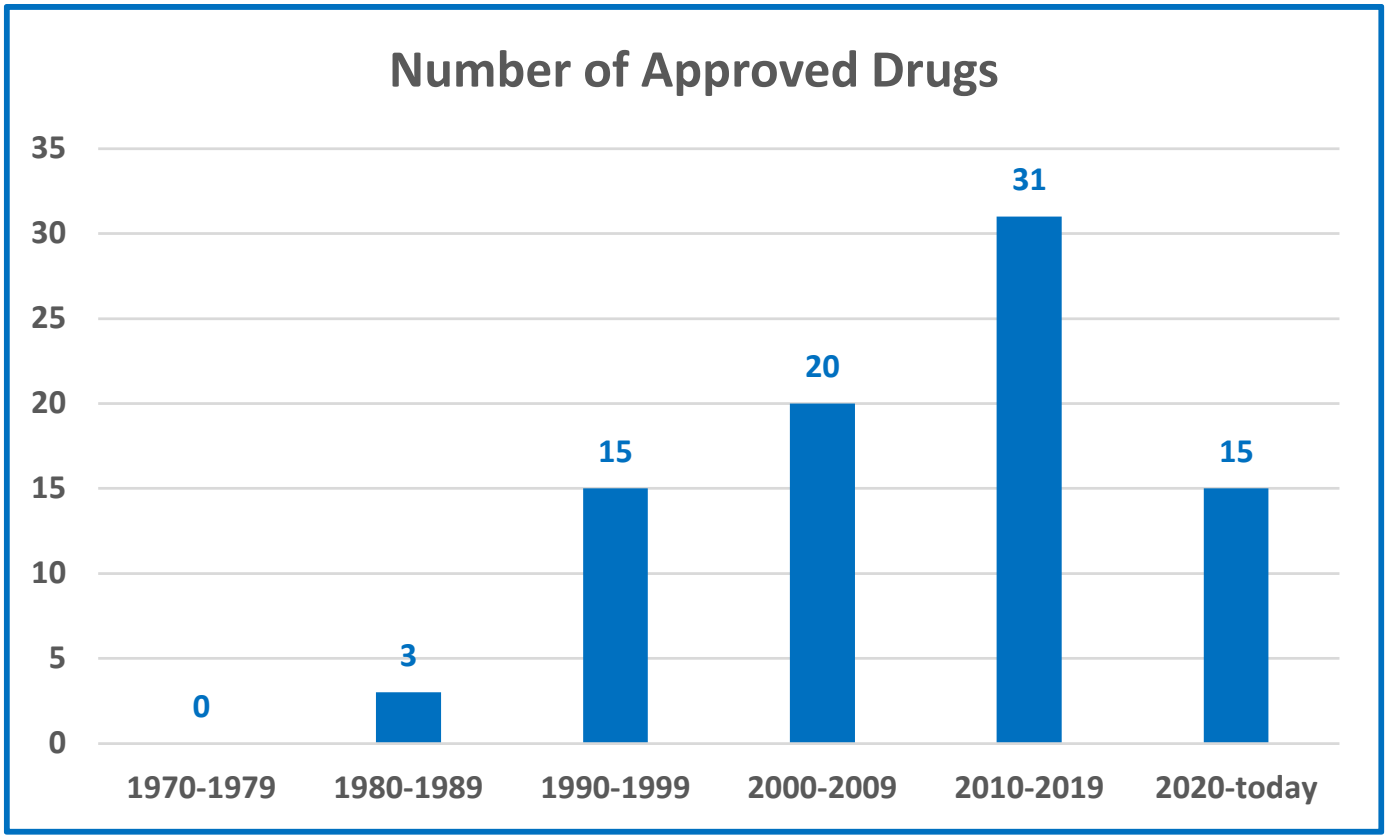

The number of approved drugs discovered with the help of CADD in blocks of ten-year periods since 1970.

CANCER

- Cancer is the leading cause of death worldwide, accounting for nearly 10 million deaths in 2022, or nearly one in five deaths, with 20 million new cancer cases diagnosed worldwide.
- 70% of cancer deaths occur in low-to-middle income countries.
- Around one-third of deaths from cancer are due to tobacco use, high body mass index, alcohol consumption, low fruit and vegetable intake, and lack of physical activity.
- Millions of lives could be saved each year by implementing resource appropriate strategies for prevention, early detection and treatment.
- By 2050, new cancer cases are expected to rise to 35 million annually, driven by population aging, growth, and lifestyle factors like obesity and smoking.

Chemosensors and Sensing Materials

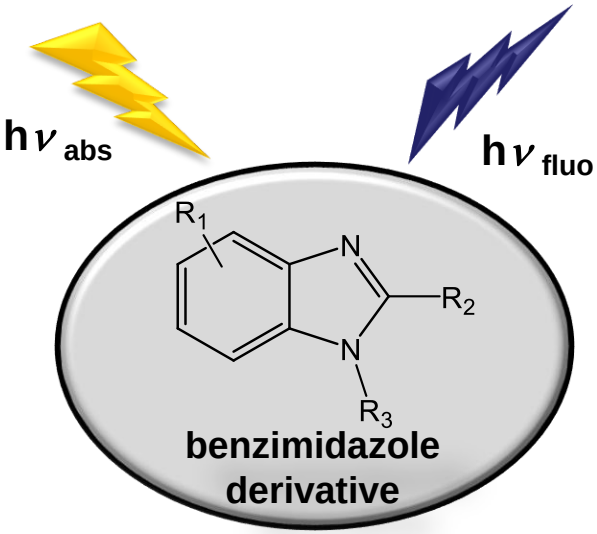

ion sensing
pH sensing

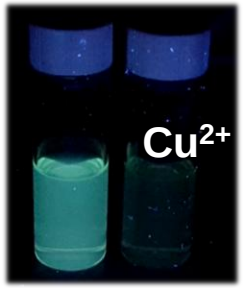

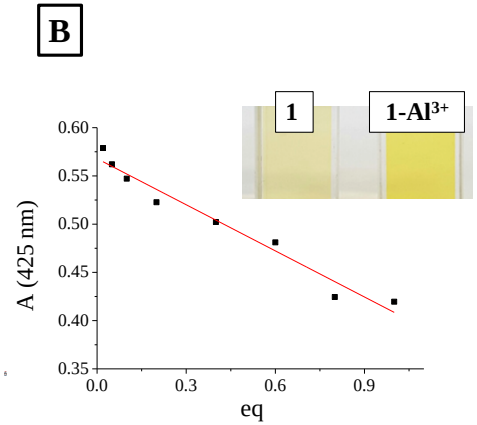

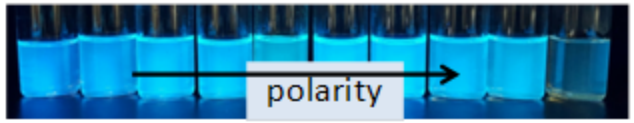

functional
(nano)materials

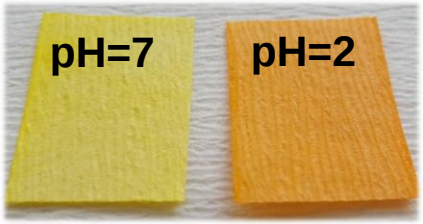

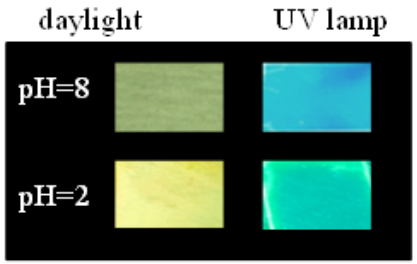

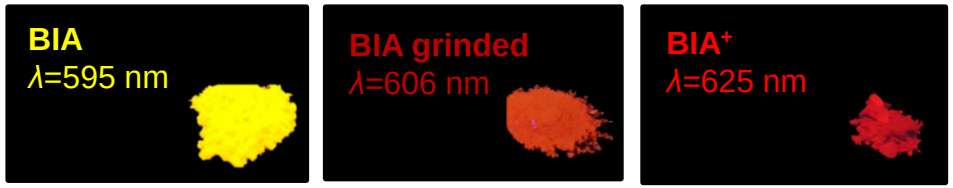

HRZZ
Croatian Science Foundation

iNFiNiTE–SENS (2015–2019)

BenzpHSens (2021–2025)

Benzimidazole based acrylonitriles

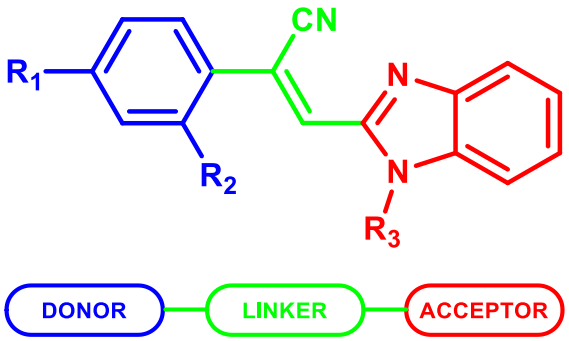

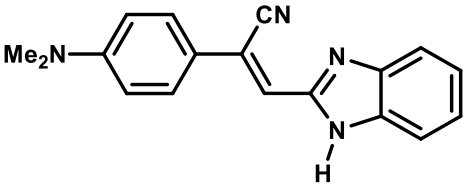

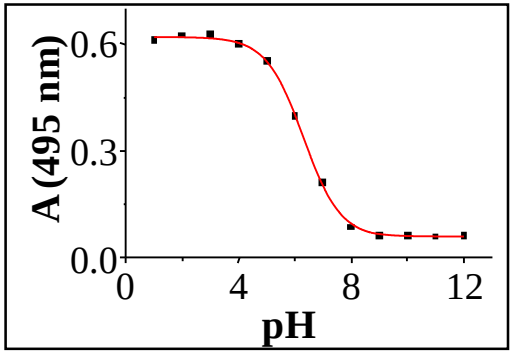

pH response

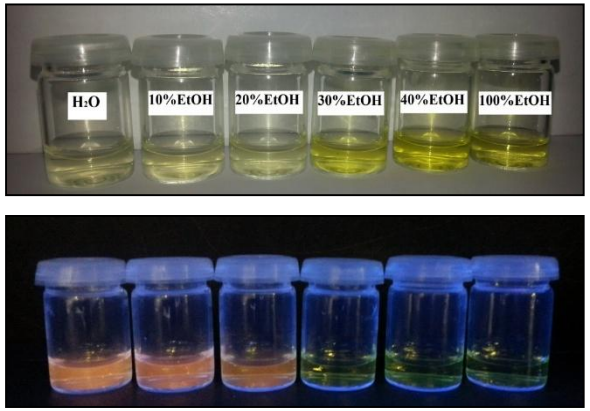

Solvent response

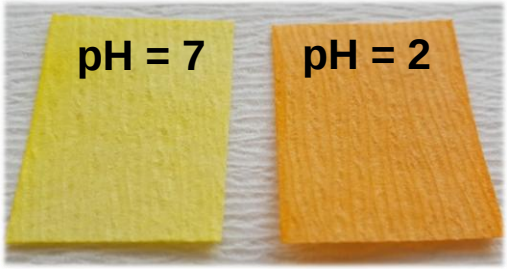

Immobilisation

Tubulin polymerisation

- Microtubules are cytoskeletal polymers essential for the maintenance of cell shape, division, migration and ordered intracellular transport, **built by heterodimers of globular α- and β-tubulin subunits**.
- The importance of microtubules in mitosis and cell division makes them a superb **target for a group of chemically diverse anticancer drugs**, such as taxol and vinblastine, as well as many others.
- Most of the drugs are antimitotic agents and inhibit cell proliferation by suppression of microtubule dynamics during the particularly vulnerable mitotic stage of the cell cycle.

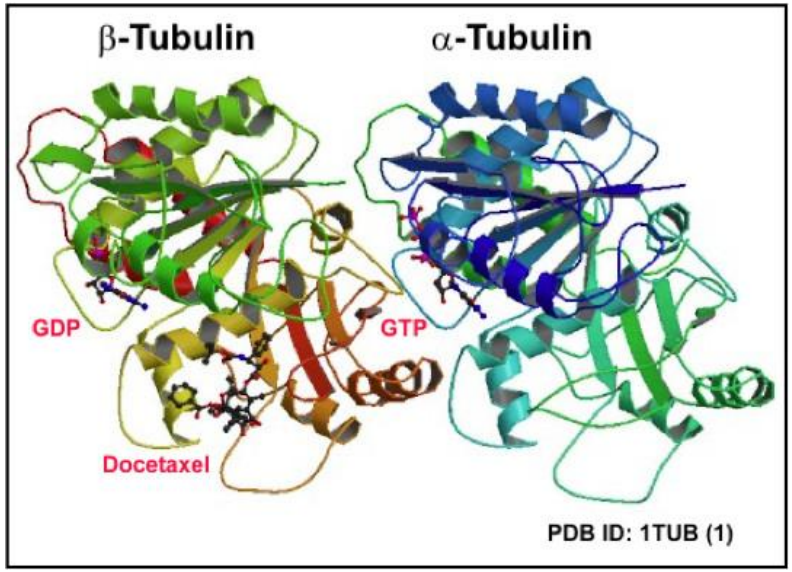

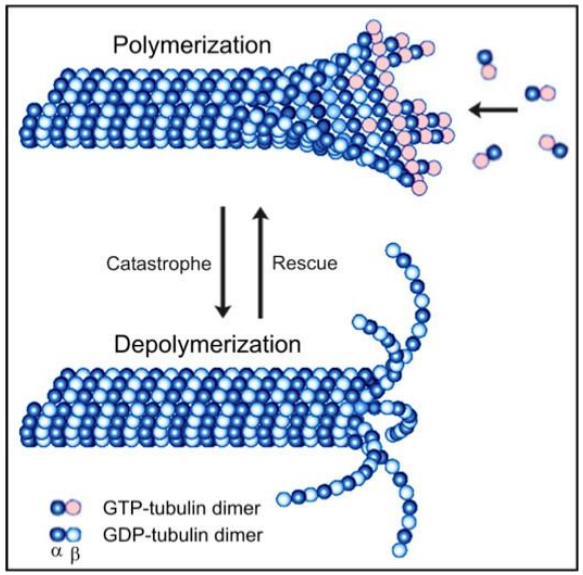

Clinical drugs targetin tubulin (de)polymerisation

Microtubule-Destabilizing Agents

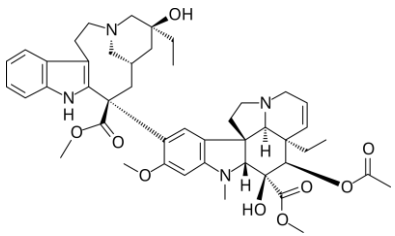

Vinblastine (1961) – Hodgkin's lymphoma, testicular cancer, and breast cancer. ($K_d \approx$ 1–2 μM)

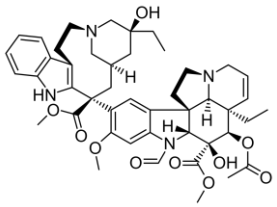

Vincristine (1963) – Acute lymphoblastic leukemia, lymphomas, and pediatric cancers. ($K_d \approx$ 1–3 μM)

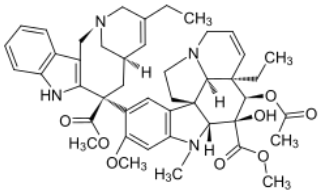

Vinorelbine (1994) – Non-small cell lung cancer and metastatic breast cancer. ($K_d \approx$ 0.1–1 μM)

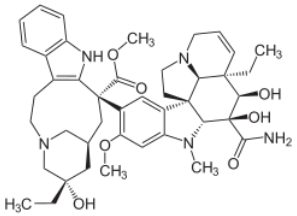

Vindesine (2012) – Acute lymphoblastic leukemia and lung cancer. ($K_d \approx$ 1–5 μM)

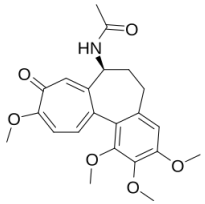

Colchicine (1961) – Explored for many cancer therapies. ($K_d \approx$ 0.1–1 μM)

Microtubule-Stabilizing Agents

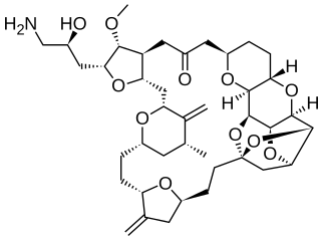

Eribulin (Halaven) (2010) – Metastatic breast cancer and liposarcoma. ($K_d \approx$ 370 nM)

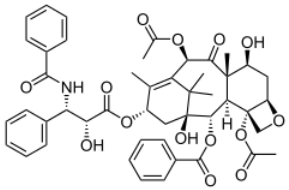

Paclitaxel (Taxol) (1998) – Breast, ovarian, lung, and pancreatic cancers. ($K_d \approx$ 10–20 nM)

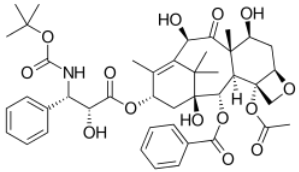

Docetaxel (Taxotere) (1996) – Breast, prostate, and lung cancers. ($K_d \approx$ 1–10 nM)

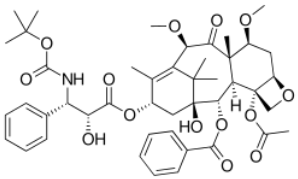

Cabazitaxel (2010) – prostate cancer, particularly in patients resistant to docetaxel. ($K_d \approx$ 10–50 nM)

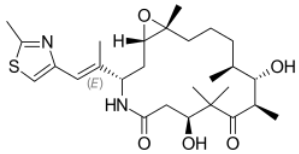

Ixabepilone (2007) – Metastatic breast cancer, especially in taxane-resistant cases. ($K_d \approx$ 70–100 nM)

BIOLOGICAL EVALUATION: Antiprolifrative activity *in vitro* (IC_{50} / μM)

Cell lines	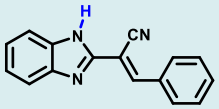	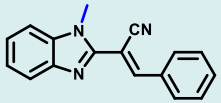	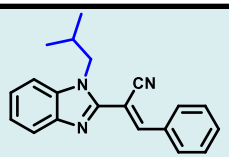	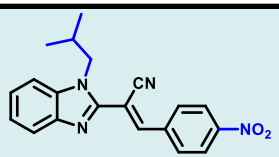	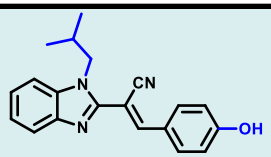	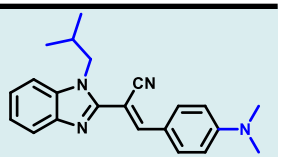
Capan-1 pancreatic adenocarcinoma	>87.5	>64.1	20.6	30.3	1.1	**0.3**
HTC-116 colorectal carcinoma	>100	>100	42.4	50.4	1.7	**0.6**
NCI-H460 lung carcinoma	>100	>100	26.1	14.8	14.0	**0.4**
DND-41 acute lymphoblastic leukemia	>100	>100	60.0	54.6	3.7	**0.2**
HL-60 acute myeloid leukemia	>100	>39.1	29.1	33.4	1.7	**0.3**
K-562 chronic myeloid leukemia	>100	>74.2	53.4	>100	49.6	4.3
LN-229 brain glioblastoma	>100	>100	66.7	72.9	3.4	1.5
Z-138 non-Hodgkin lymphoma	13.7	>100	40.1	45.4	2.3	**0.4**

	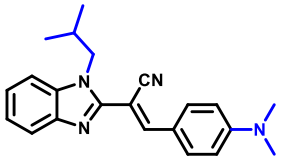	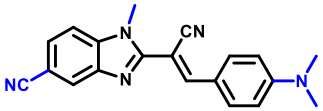	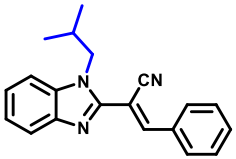	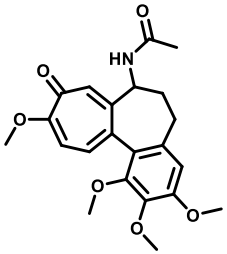
	30	**42**	**29**	**colchicine**
ΔG_{BIND} (kcal mol^{-1})	**–8.6**	**–8.1**	–8.6	**–9.3** $[-8.3]_{EXP}$
IC_{50} (μM)	0.2 – 4.3	> 56.0	20.6 – 66.7	$[0.003]_{EXP}$

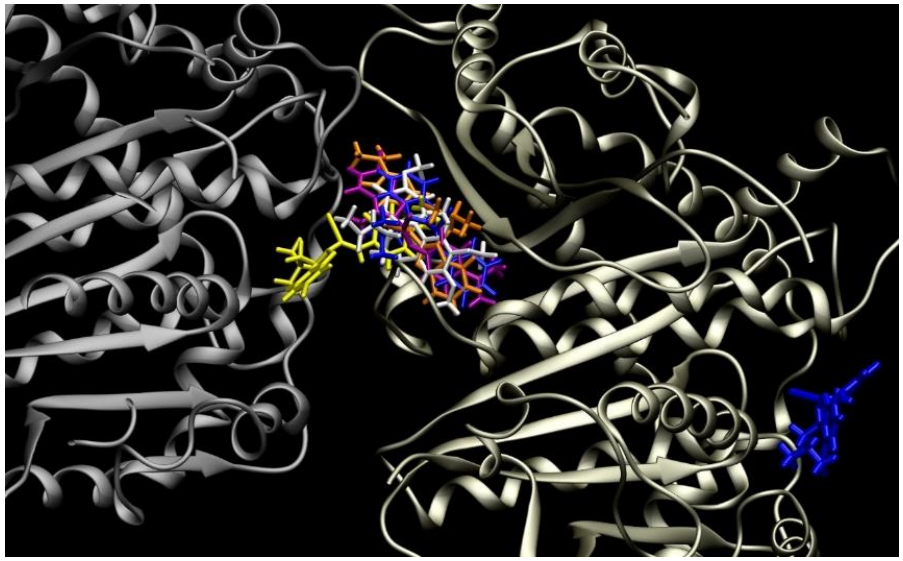

The most favourable binding position for investigated ligands. Colchicine is given in white, while other ligands are coloured in blue (**29**), orange (**30**), yellow (**41**), and purple (**42**). Tubulin's subunits are given in grey (α) and gold (β).

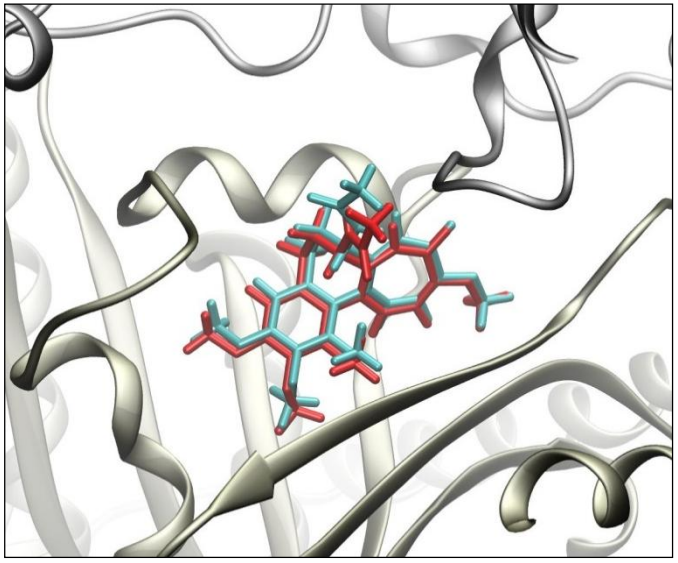

The overlap of colchicine structures as predicted through the docking procedure (in cyan) and that from the tubulin-colchicine crystal structure (in red).

The most active compound 30

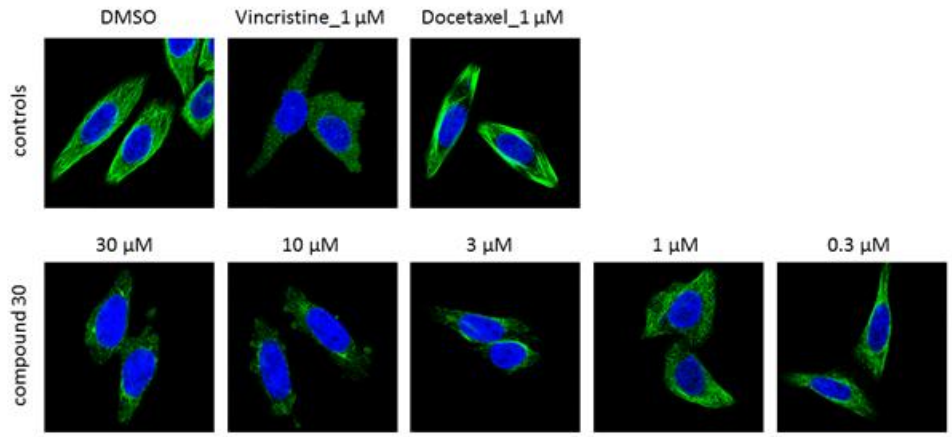

Immunofluorescence staining of α-tubulin in HEp-2 cells treated for 3 hours with indicated concentrations of system **30**, or reference compounds **vincristine** and **docetaxel**. Green: α-tubulin, blue: DAPI. Scale bar: 20 µM

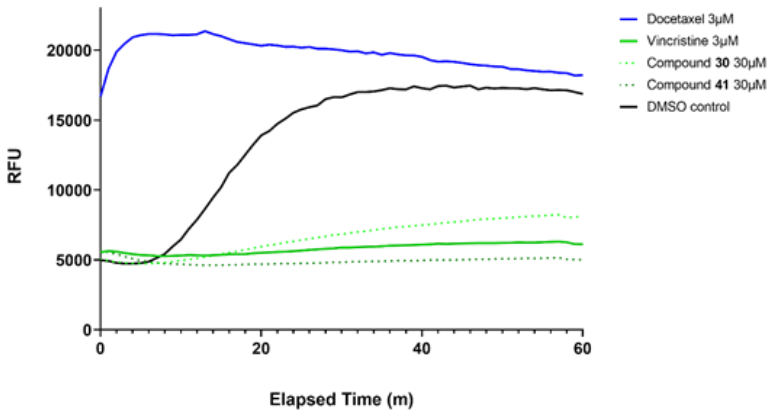

Effect of system **30** on *in vitro* tubulin polymerization. Purified porcine neuronal tubulin and GTP were mixed in a 96-well plate. **Vincristine** and **docetaxel** (3 µM) were used as reference systems, and **DMSO** as a vehicle control. The effect on tubulin assembly was recorder in a Tecan Spark multimode plate reader at 60 sec intervals for 1 hour at 37 °C. Each condition was tested in duplicate. Polymerization was measured by monitoring the excitation at 350 nm and emission at 435 nm.

CONCLUSIONS

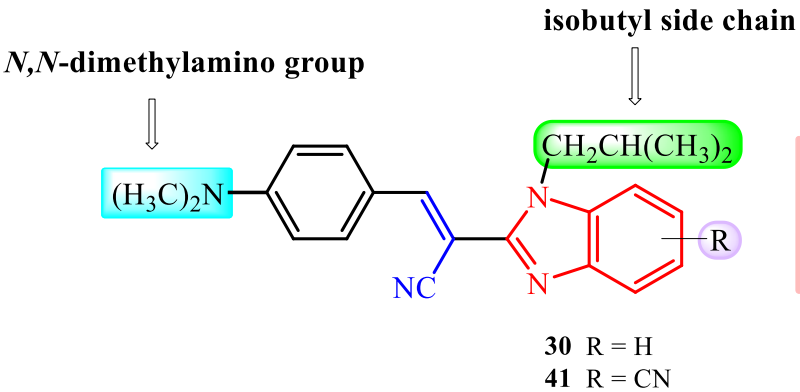

30 and 41 - the most prominent antiproliferative activity (IC_{50} = 0.6 - 0.2 μM)

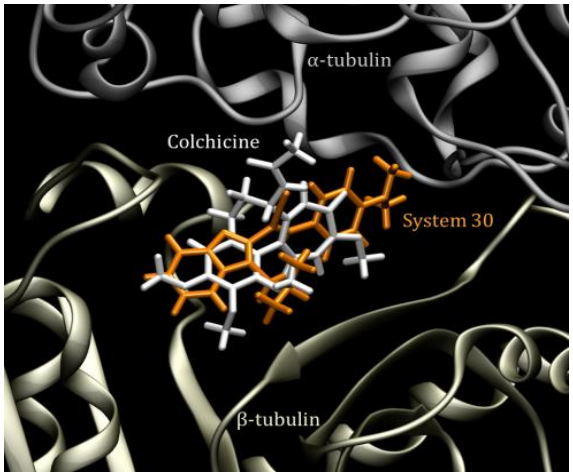

- Synthesis, biological activity and computational analysis of novel *N*-substituted benzimidazole-based acrylonitriles
- Compounds **30** and **41** show selective antiproliferative activity in submicromolar range of concentrations (IC_{50} = 0.2 – 0.6 μM)
- All compunds inhibit cancer cell proliferation by disintegrating microtubules
- *N*-isobutyl group occupies a hydrophobic pocket and ensures a proper ligand orientation
- **–NMe_2 group on the phenyl unit promotes binding through favorable hydrogen-bonding interactions with Lys352**

N Perin, L Hok, A Beč, L Persoons, E Vanstreels, D Daelemans, R Vianello, M Hranjec, *Eur J Med Chem* **2021**, *211*, 113003.

Can we replace the *p*-NMe_2 group with something else?

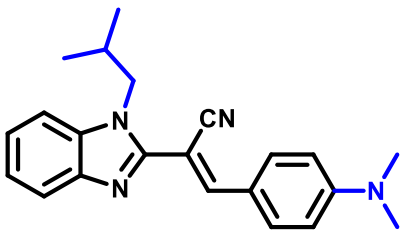

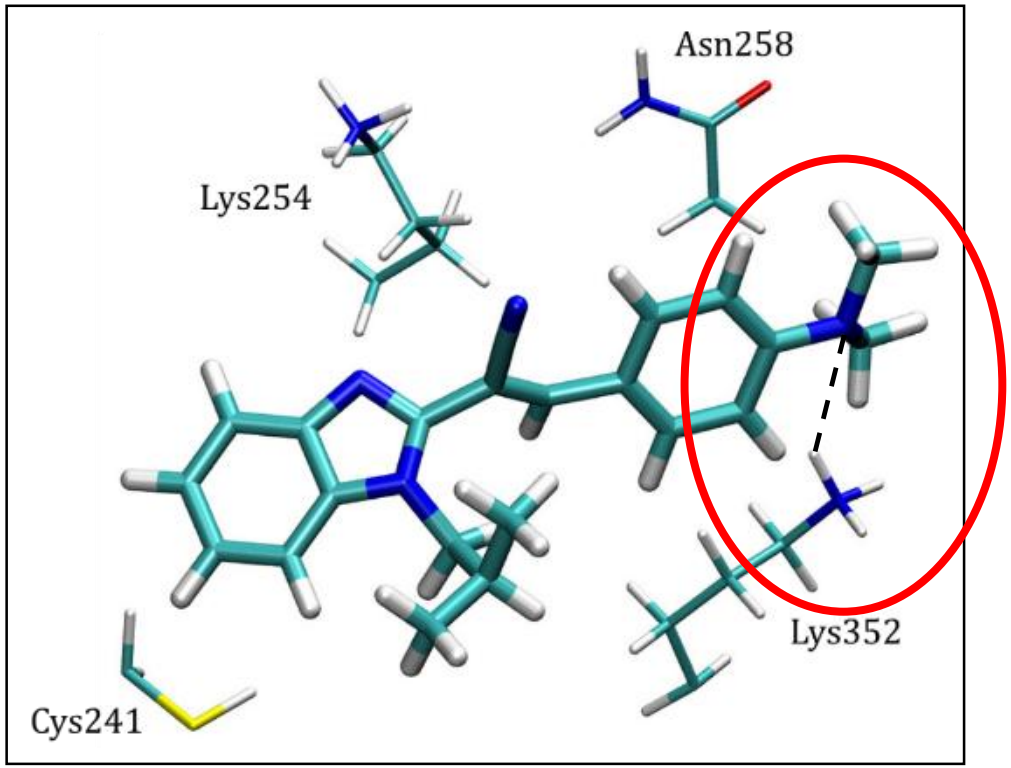

The –NMe_2 group in compound **30** forms a hydrogen bonding with **Lys352**

What about replacing *p*-NMe_2 with the *p*-NEt_2 group?

Replacing the *p*-NMe_2 group with *p*-NEt_2

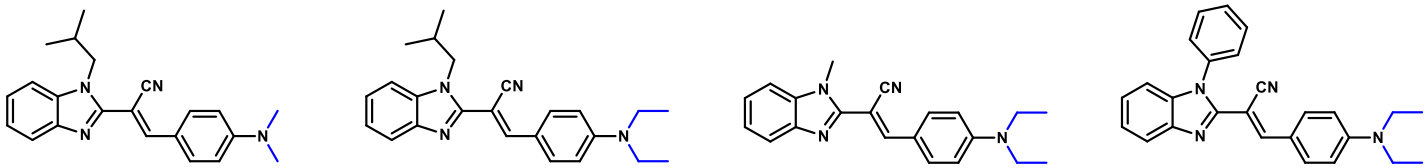

	30	64	63	66
ΔG_{BIND} (kcal mol^{-1})	−8.6	−8.7	−8.0	−8.8 (allosteric)
IC_{50} (μM)	0.2 – 4.3	1.8 – 5.9	-	> 100

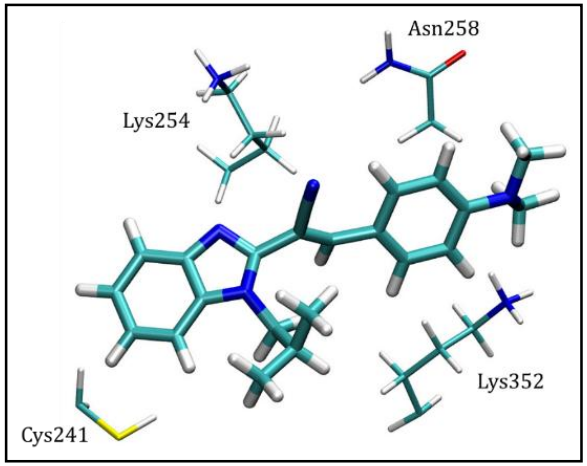

30

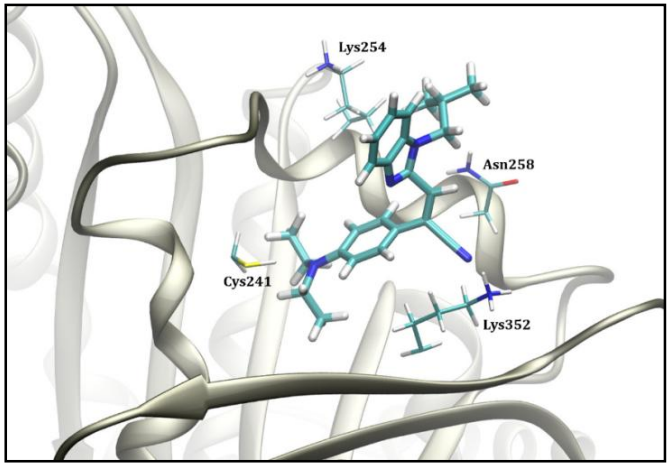

64

- The introduced *p*-NEt_2 group makes this part of the ligand too large for the most active conformation, which changes binding orientation and exhibits a somewhat reduced biological activity

Biological activity of the *E*-isomer of compound 64

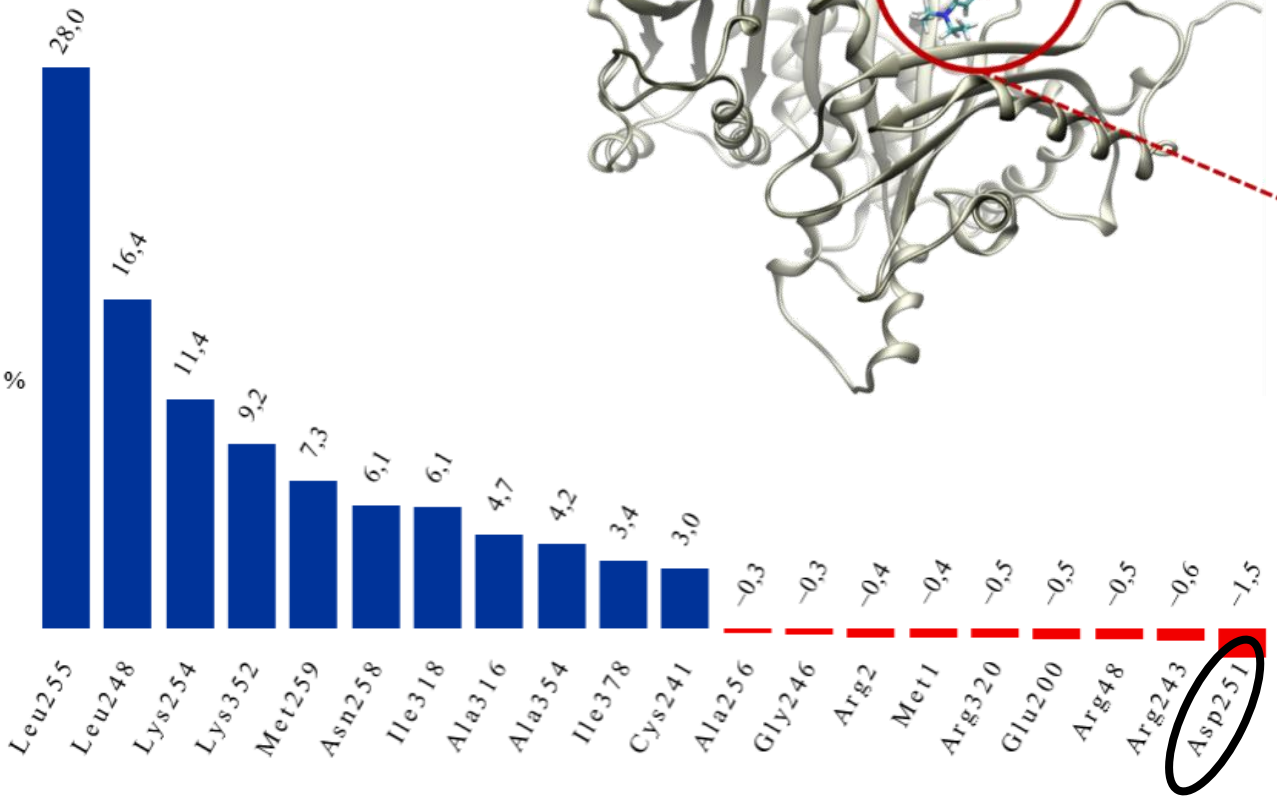

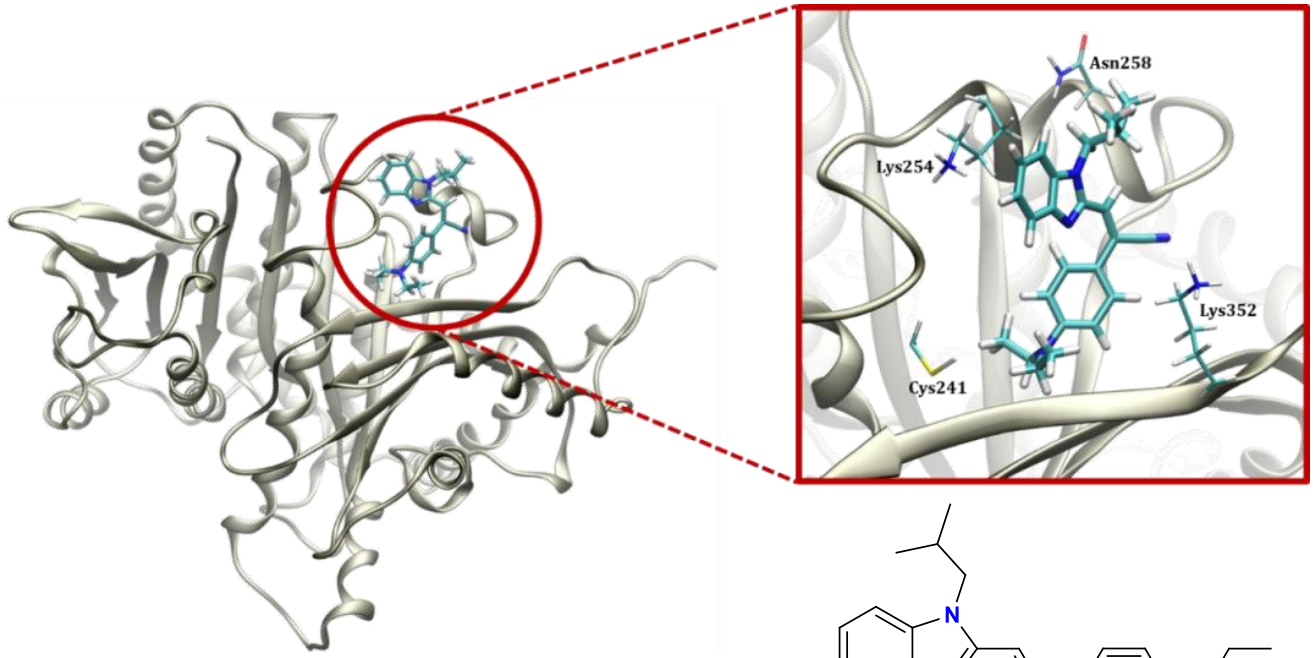

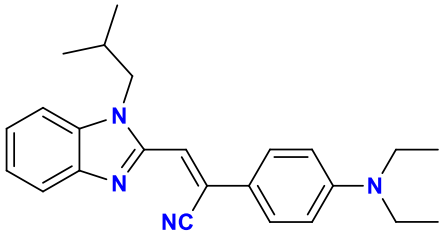

ΔG_{BIND} = –8.7 kcal mol^{-1}

How is Asp251 disturbing the binding?

How is Asp251 disturbing the binding?

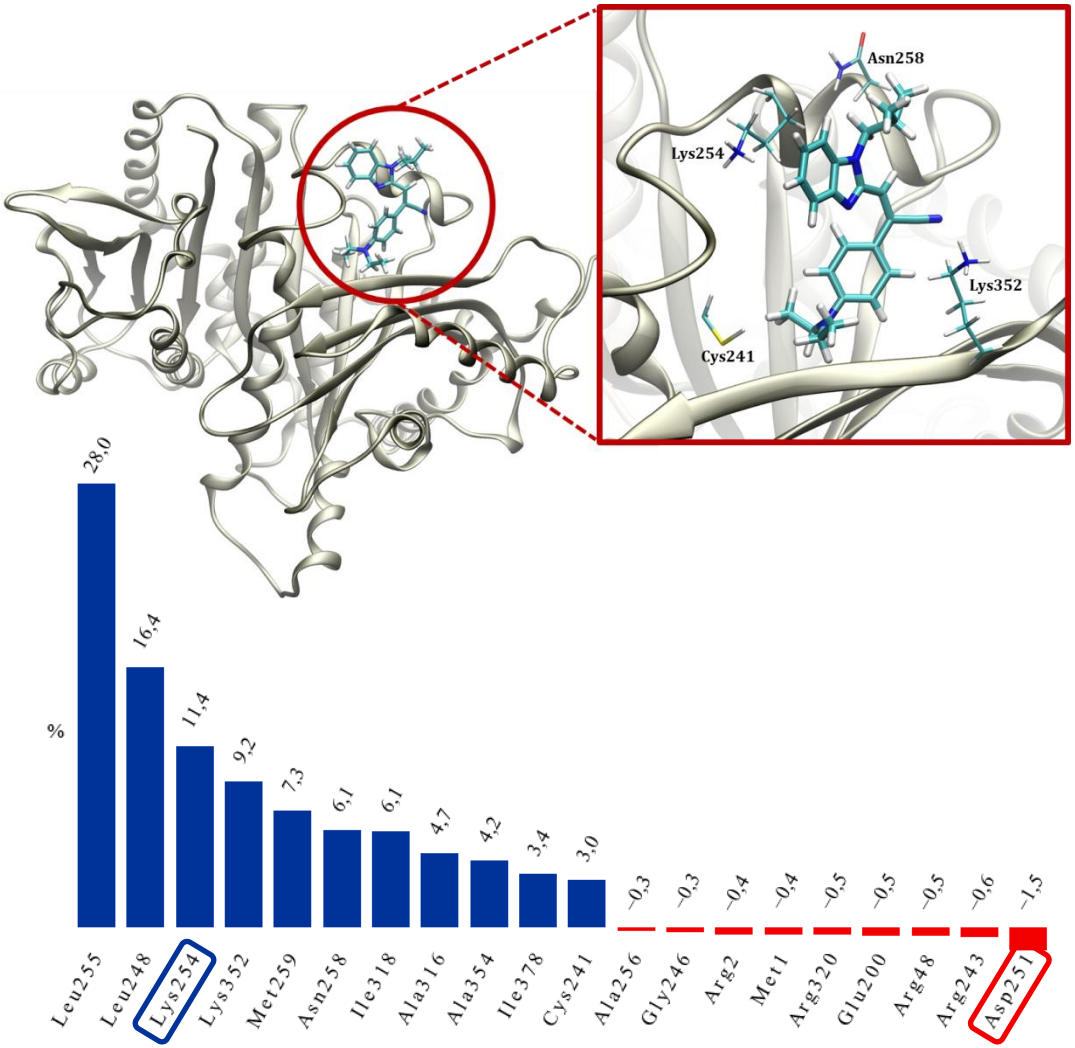

Asp251···Lys254 interactions during
20% of the simulation time

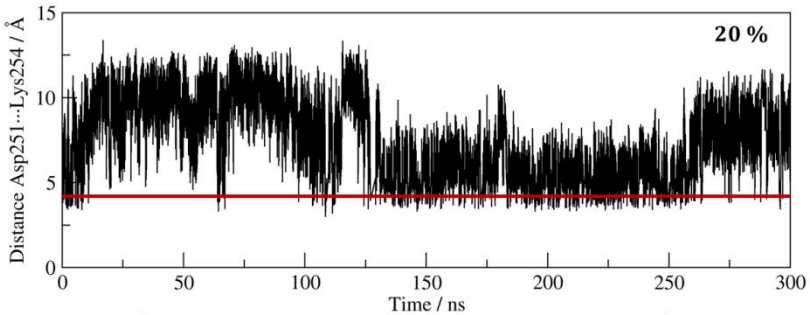

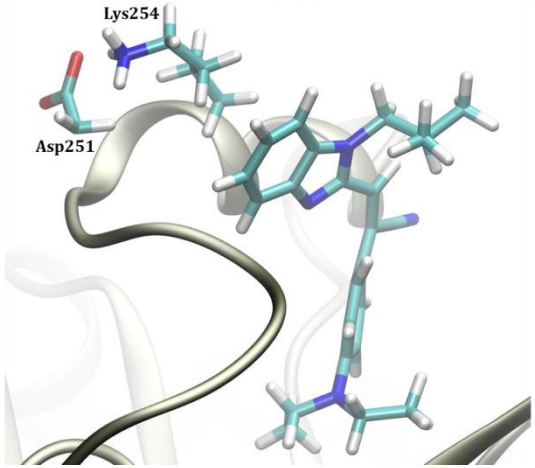

How is Asp251 disturbing the binding?

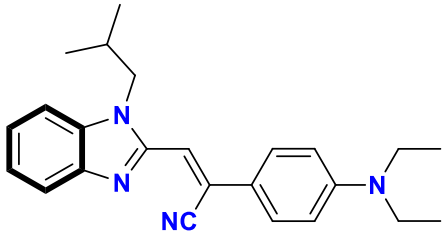

Asp251···Lys254 interactions during
20% of the simulation time

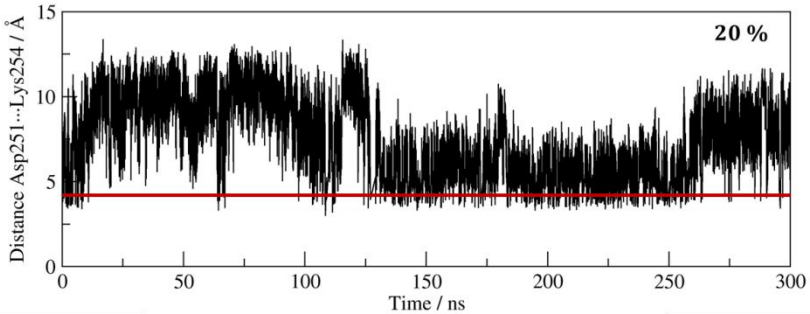

COO⁻(Asp251)·····**phenyl**(benzimidazole) distance

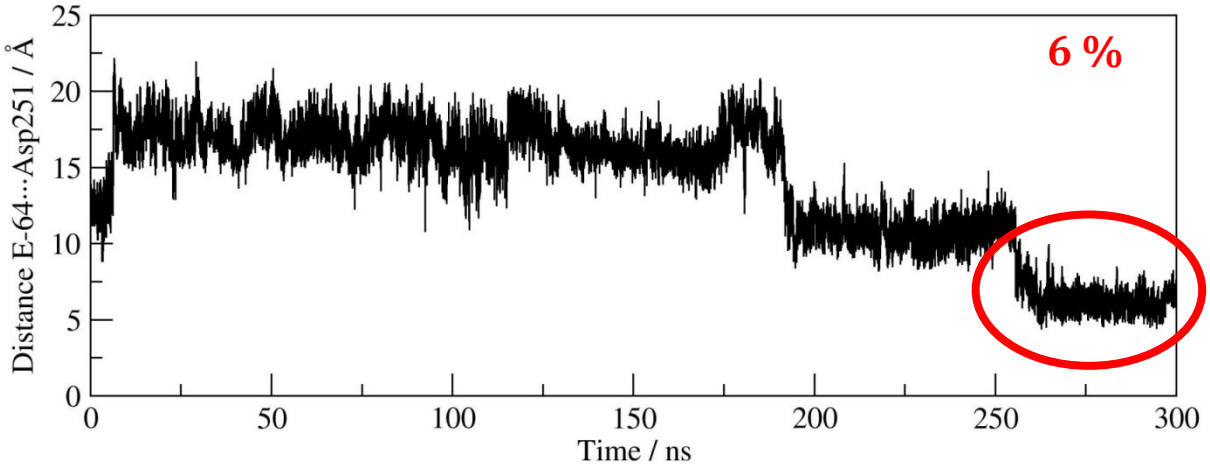

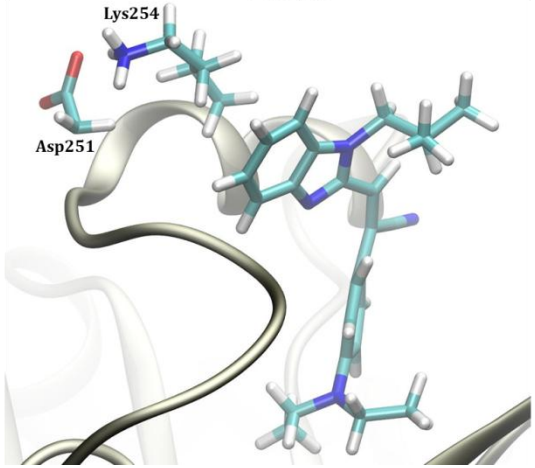

- During 6% of the simulation time, **COO⁻** group from Asp251 approaches the **phenyl** group of the benzimidazole unit and establishes **unfavorable interactions**

How is Asp251 disturbing the binding?

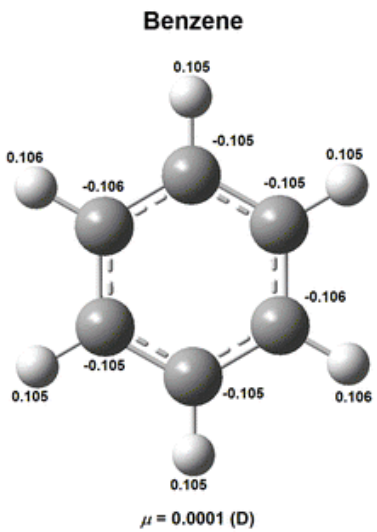

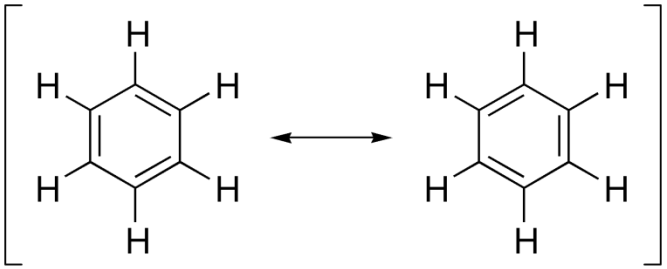

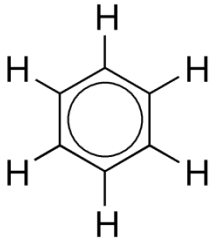

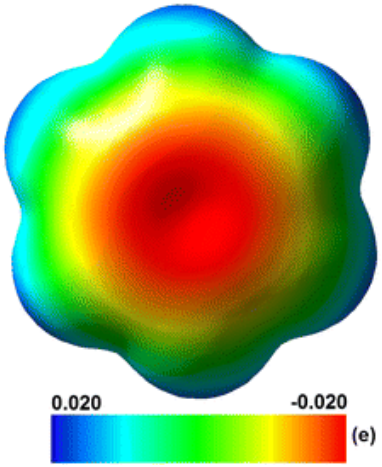

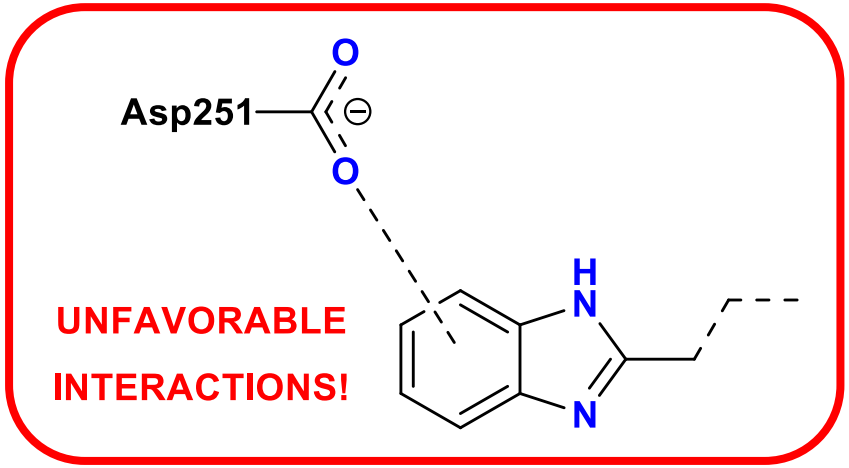

How is Asp251 disturbing the binding?

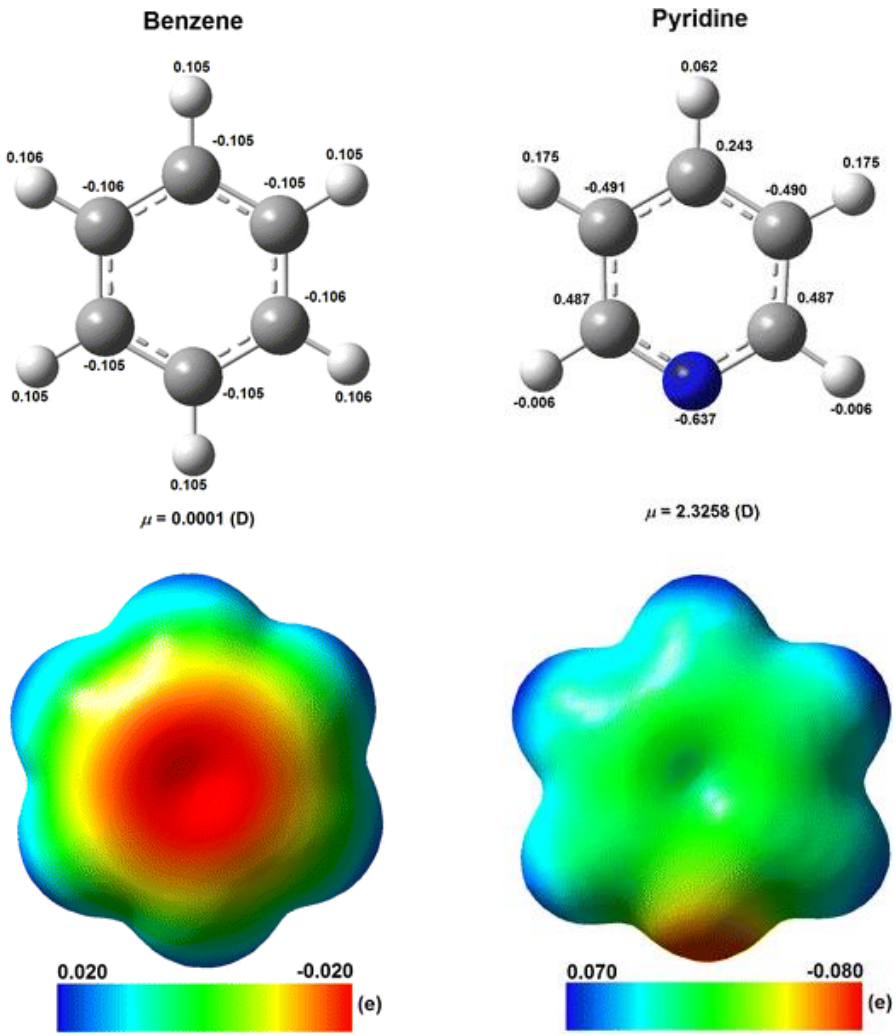

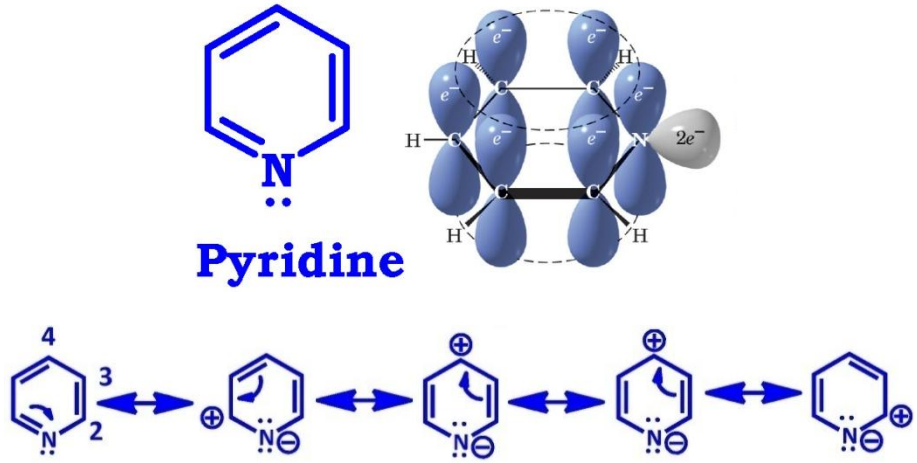

The obtained insight suggested replacing **benzimidazole** with **imidazo[4,5-*b*]pyridine** as a potentially useful strategy.

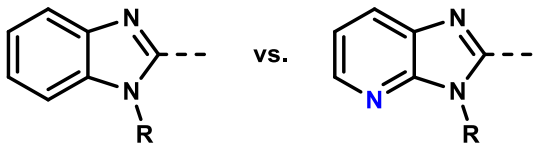

Computer-Aided Drug Design

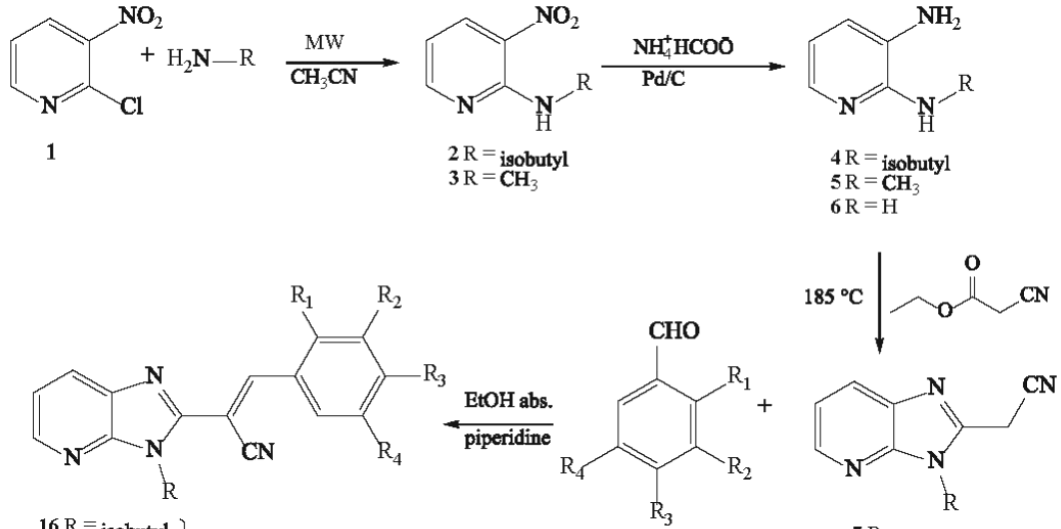

Marijana Hranjec
FCET, Zagreb

Ida Boček
FCET, Zagreb

Anja Beč
FTT, Zagreb

Biological activity of imidazo[4,5-*b*]pyridine based acrylonitriles

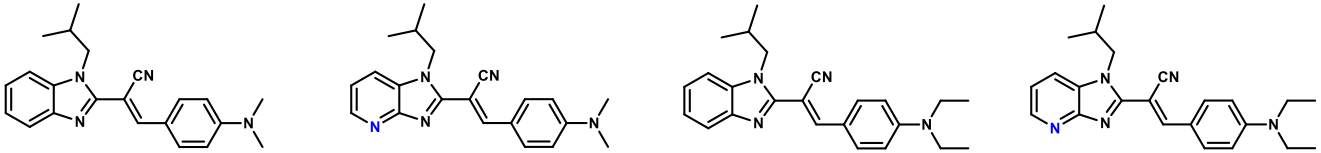

	30	30a	64	64a
ΔG_{BIND} (kcal mol^{-1})	-8.6	-6.9	-8.7	-6.6
IC_{50} (μM)	0.2 – 4.3	0.3 – 6.5	1.8 – 5.9	0.2 – 2.5

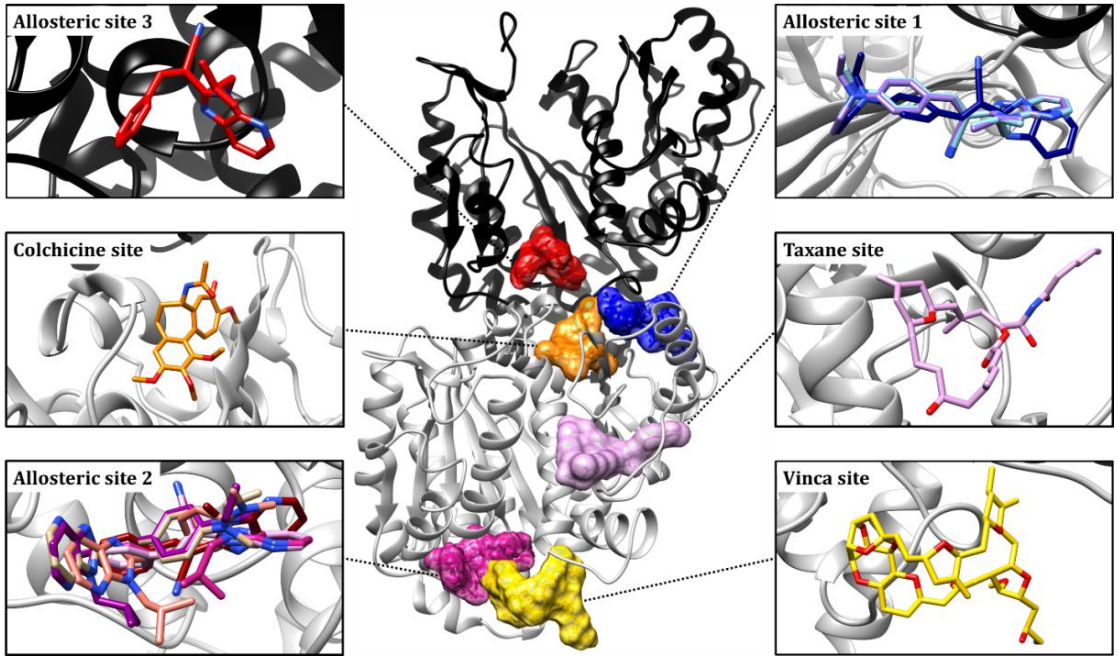

- *E*-isomers of **30a** and **64a** bind to the **allosteric site 1** (in blue), while the matching inset gives their overlapped position in light blue and purple, respectively.
- **Colchicine** (in orange), **taxane** (in pink) and **vinca** sites (in yellow) are visualized based on the position of the appropriate ligands in the corresponding 5EYP, 4I4T and 5JH7 crystal structures on the α- (in black) and β-subunits (in gray) in the tubulin dimer.

Biological activity of imidazo[4,5-*b*]pyridine based acrylonitriles

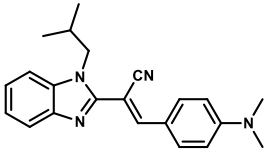

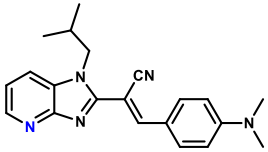

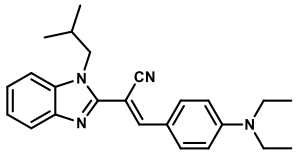

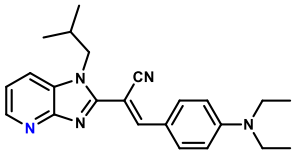

	30	30a	64	64a
ΔG_{BIND} (kcal mol^{-1})	-8.6	-6.9	-8.7	-6.6
IC_{50} (μM)	0.2 – 4.3	0.3 – 6.5	1.8 – 5.9	0.2 – 2.5

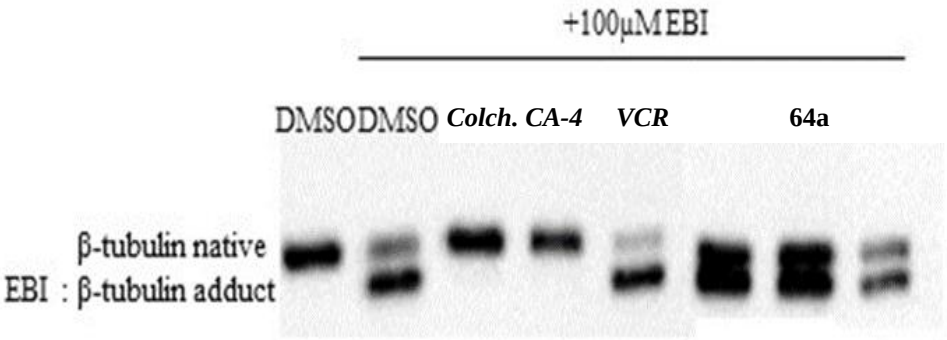

Western blot analysis shows that **64a** does not inhibit the formation of the EBI:β-tubulin adduct, which confirms it does not bind within the **colchicine binding site**.

Compound	IC_{50} / μM PBMC	
	Donor 1	Donor 2
64a	>100	>100
Docetaxel	>0,1	>0,1
Vincristine	>0,1	>0,1

Toxicity of **64a** on normal PBMC cells.

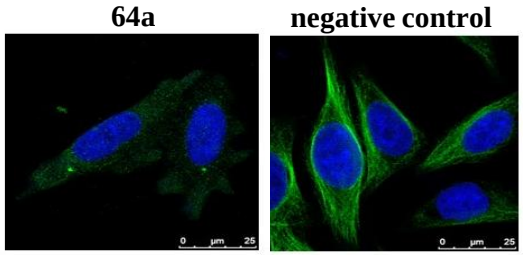

Immunofluorescence staining of α-tubulin in HEp-2 (human cervix carcinoma) cells treated for 3 hours. Green: α-tubulin, blue: DAPI.

Biological activity of imidazo[4,5-*b*]pyridine based acrylonitriles

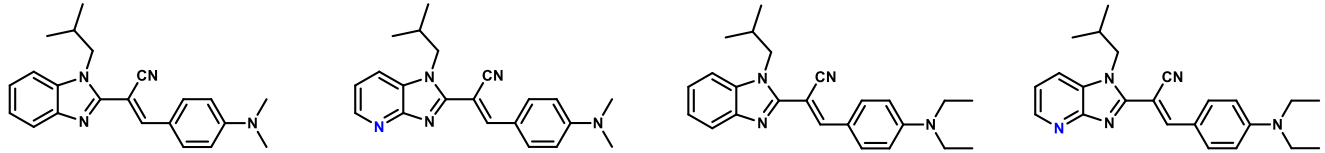

	30	30a	64	64a
ΔG_{BIND} (kcal mol^{-1})	-8.6	-6.9	-8.7	-6.6
IC_{50} (μM)	0.2 – 4.3	0.3 – 6.5	1.8 – 5.9	0.2 – 2.5

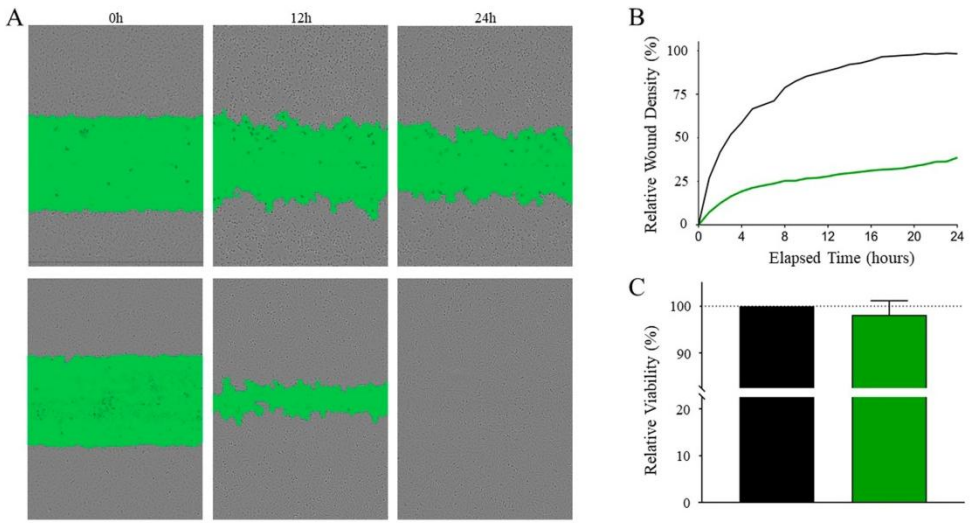

Effect of **64a** on cancer cell migration. (A) Image of a scratch wound assay in LN-229 cells incubated with 0.5 μM of **64a** (top) or left untreated (bottom). Scratch wound area is marked in green. (B) Wound closure expressed as the relative wound density, monitored for 24 h. Migration curve for the untreated control is shown in black, **64a** is shown in green. (C) Bar graphs showing the relative viability of cells at time point 24 h, with the untreated control set to 100.

Biological activity of compound 64a

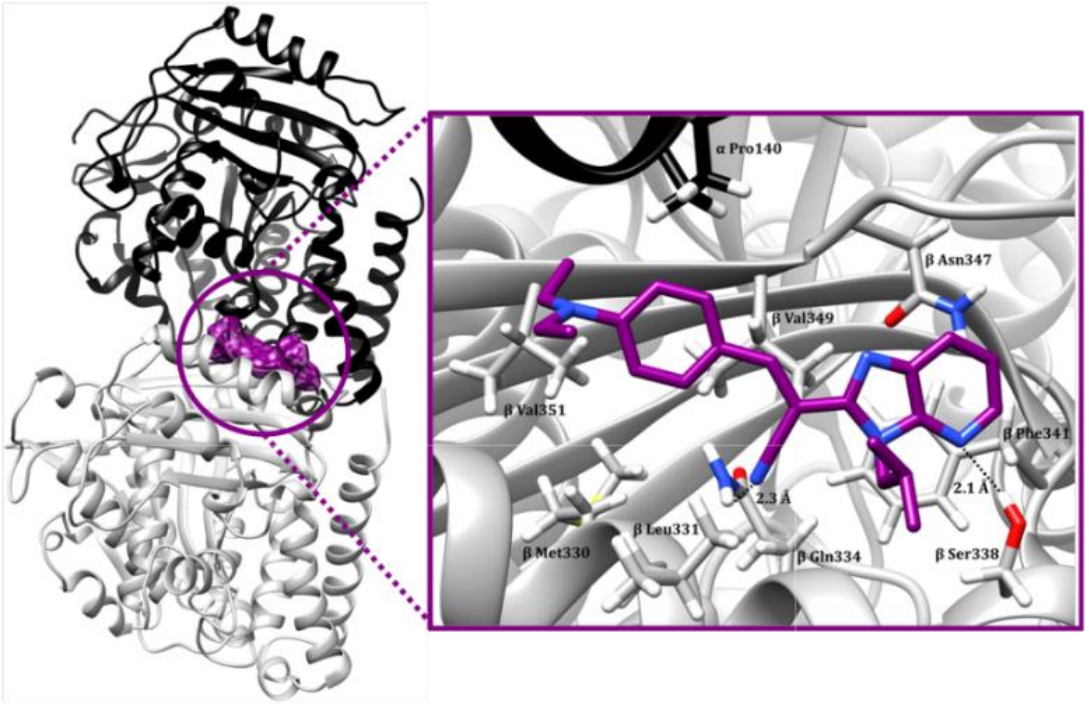

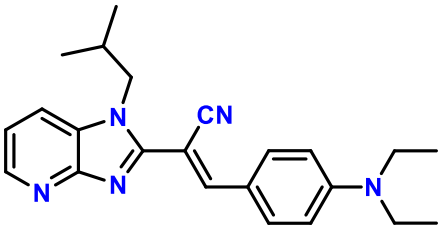

E-isomer (0.0) vs. *Z*-isomer (+4.2)

$\Delta G_{BIND} = -6.6$ kcal mol^{-1}

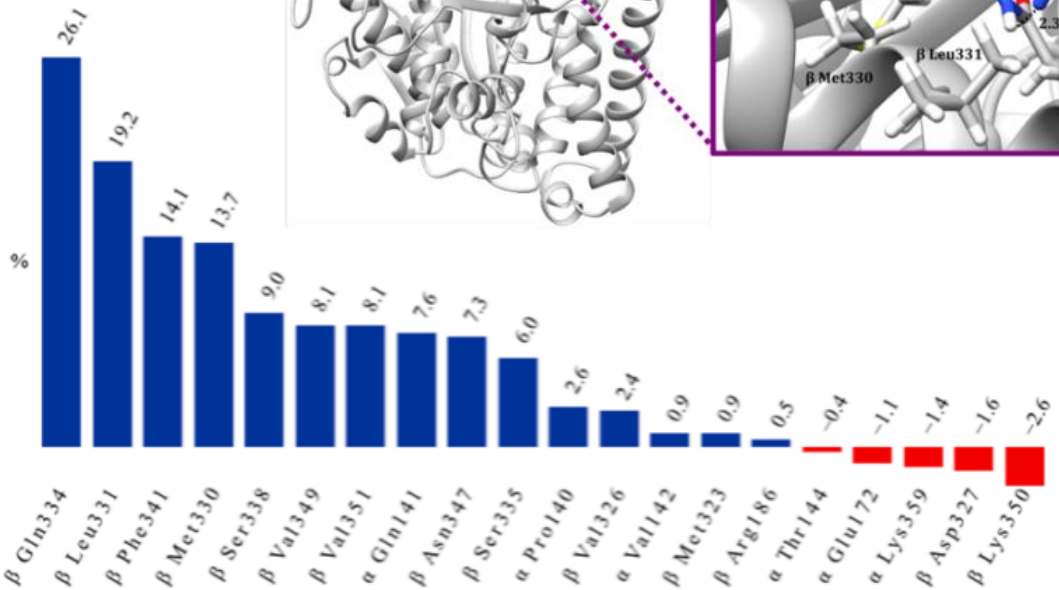

N. Perin, L. Hok, A. Beč, L. Persoons, E. Vanstreels, D. Daelemans, R. Vianello, M. Hranjec, *European Journal of Medicinal Chemistry* **2021**, *211*, 113003.

A. Beč, L. Hok, L. Persoons, E. Vanstreels, D. Daelemans, R. Vianello, M. Hranjec, *Pharmaceuticals* **2021**, *14*, 1052.

I. Boček, L. Hok, L. Persoons, D. Daelemans, R. Vianello, M. Hranjec, *Bioorganic Chemistry* **2022**, *127*, 106032.

Biological activity of imino-coumarin and 2-benzazole hybrids

Cell lines	Capan-1 pancreatic adenocarcinoma	HTC-116 colorectal carcinoma	NCI-H460 lung carcinoma	DND-41 acute lymphoblastic leukemia	HL-60 acute myeloid leukemia	K-562 chronic myeloid leukemia	LN-229 brain glioblastoma	Z-138 non-Hodgkin lymphoma
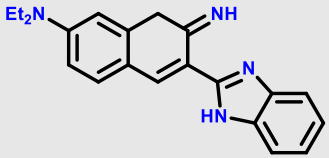	>100	>100	>100	>100	>100	>100	>68.3	>100
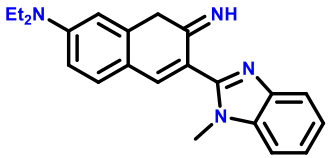	**0.07**	**0.1**	**0.1**	**0.07**	**0.06**	**0.05**	**0.1**	**0.07**
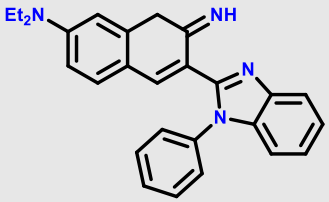	>100	>100	>100	>100	>100	>100	20.6	>100
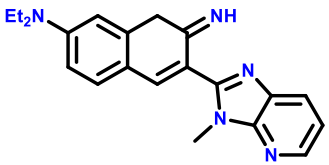	26.6	>100	>100	21.6	50.3	28.6	>100	52.2

I Boček Pavlinac, L Persoons, A Beč, L Vrban, D Daelemans, R Vianello, M Hranjec, *Bioorg Chem* **2025**, *154*, 107991.

Acknowledgement

Lucija Vrban
Ruđer Bošković Institute
Zagreb, Croatia

Tana Tandarić
Ruđer Bošković Institute
Zagreb, Croatia

Tamara Rinkovec
Ruđer Bošković Institute
Zagreb, Croatia

Lucija Hok
University of Cincinnati
College of Medicine, USA

Janez Mavri
National Institute of Chemistry
Ljubljana, Slovenia

Jernej Stare
National Institute of Chemistry
Ljubljana, Slovenia

Marijana Hranjec
FCET University of Zagreb
Zagreb, Croatia

Ida Boček
FCET University of Zagreb
Zagreb, Croatia

Anja Beč
FTT University of Zagreb
Zagreb, Croatia

Dirk Daelemans
Microbiology Department
KU Leuven, Belgium

Leentje Persoons
Microbiology Department
KU Leuven, Belgium

Lynn Kamerlin
Chemistry & Biochemistry
Georgia Tech., USA